

AJTEC2011-44343

**DRAFT: THERMAL PROPERTIES OF YTTRIUM ALUMINUM GARNETT FROM
MOLECULAR DYNAMICS SIMULATIONS**

Majid S. al-Dosari *

Thermal Engineering Laboratory
Department of Mechanical Engineering
Vanderbilt University
Nashville, Tennessee 37235
majid.s.aldosari@vanderbilt.edu

Don G. Walker

Thermal Engineering Laboratory
Department of Mechanical Engineering
Vanderbilt University
Nashville, Tennessee, 37235
greg.walker@vanderbilt.edu

ABSTRACT

Yttrium Aluminum Garnet (YAG, $Y_3Al_5O_{12}$) and its varieties have applications in thermographic phosphors, lasing mediums, and thermal barriers. In this work, thermal properties of crystalline YAG where aluminum atoms are substituted with gallium atoms ($Y_3(Al_{1-x}Ga_x)_5O_{12}$) are explored with molecular dynamics simulations. For YAG at 300°K, the simulations gave values close to experimental values for constant-pressure specific heat, thermal expansion, and bulk thermal conductivity. For various values of x , the simulations predicted no change in thermal expansion, an increase in specific heat, and a decrease in thermal conductivity for $x=50\%$. Furthermore, the simulations predicted a decrease in thermal conductivity with decreasing system size.

NOMENCLATURE

A two-body potential parameter
 B two-body potential parameter
 E total energy
 E_{TS} change in system energy due to a thermostat
 E_{TS}^{avg} average of the absolute values of E_{TS}
 T temperature
 U potential energy
 V volume
 V_0 initial volume
 a lattice spacing
 c_p constant-pressure specific heat

c_v constant-volume specific heat
 k thermal conductivity
 q elementary charge
 \dot{q} heat flux
 r_{ij} distance between atoms i and j
 $r_{0,ij}$ atomic bonding cutoff between atoms i and j
 t time
 x fraction of Al randomly substituted with Ga:
 $Y_3(Al_{1-x}Ga_x)_5O_{12}$
 Λ mean free path
 Ω three-body angular expression
 α thermal expansion
 γ three-body potential parameter energy
 λ three-body potential parameter
 θ_{jik} angle \widehat{jik}
 θ_0 three-body potential parameter

Introduction

Yttrium Aluminum Garnet (YAG, $Y_3Al_5O_{12}$) is a synthetic crystal with a complicated atomic structure. Doped varieties are used for solid state lighting, as thermographic phosphors, in thermal barriers, and as lasing mediums. The inherent thermal design issues of these systems motivate the study of the thermal transport of YAG.

Since YAG has a relatively low thermal conductivity, its thermal transport is primarily governed by phonons which are inferred from atomic motion. Therefore, molecular dynamics

* Address all correspondence to this author.

TABLE 1. THERMAL PROPERTIES CRYSTALLINE OF YAG

Melting Temperature, T_m	2213 K [2]
Thermal Expansion, α	$7.0 \cdot 10^{-6} \text{ K}^{-1}$ @ 300 K [3]
Specific Heat, c_p	$0.6 \text{ J} \cdot \text{g}^{-1} \text{ K}^{-1}$ [4] [5]
Thermal Conductivity, k	$10\text{--}14 \text{ W} \cdot \text{m}^{-1} \text{ K}^{-1}$ [6]

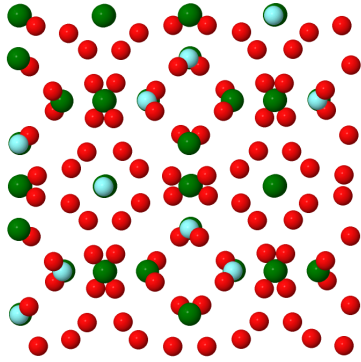


FIGURE 1. CONVENTIONAL UNIT CELL YAG SYMMETRY ON [1 0 0] FACE. Red:O, Green:Al, Blue:Y. (Image generated by Jmol [9])

(MD) simulations can offer insight into the thermal properties of YAG of varying system parameters.

In the work introduced by Hansel [1], gallium is substituted for aluminum in various percentages to study its effect on luminescence. In this work, aluminum substitution with gallium will be a variable to study its effect on constant-pressure specific heat, lattice constant, thermal expansion, and thermal conductivity. In addition, system size will be introduced as a variable for thermal conductivity.

Thermal properties of pure, crystalline YAG are reported in Table 1 to be compared against results from the simulations.

YAG Model

YAG crystallizes in a highly symmetric cubic structure (detailed in Ref. [7]). The conventional unit cell of YAG contains 160 atoms comprising of 24 yttrium, 40 aluminum, and 96 oxygen atoms; with a lattice parameter of 12.01 \AA [8]. The relative arrangement of Y, O, and Al can be described with polyhedra as shown in Fig. 2, while the symmetry can be seen in Figure 1.

Jun, et al. [10] have modeled the complex structure of pure YAG for classical molecular dynamics simulation by fitting elasticity and lattice constant data to the potential energy functions reproduced here. However, this work adapts for the purposes of this work, gallium atoms are considered substitutable for aluminum atoms, effectively representing only a change in mass.

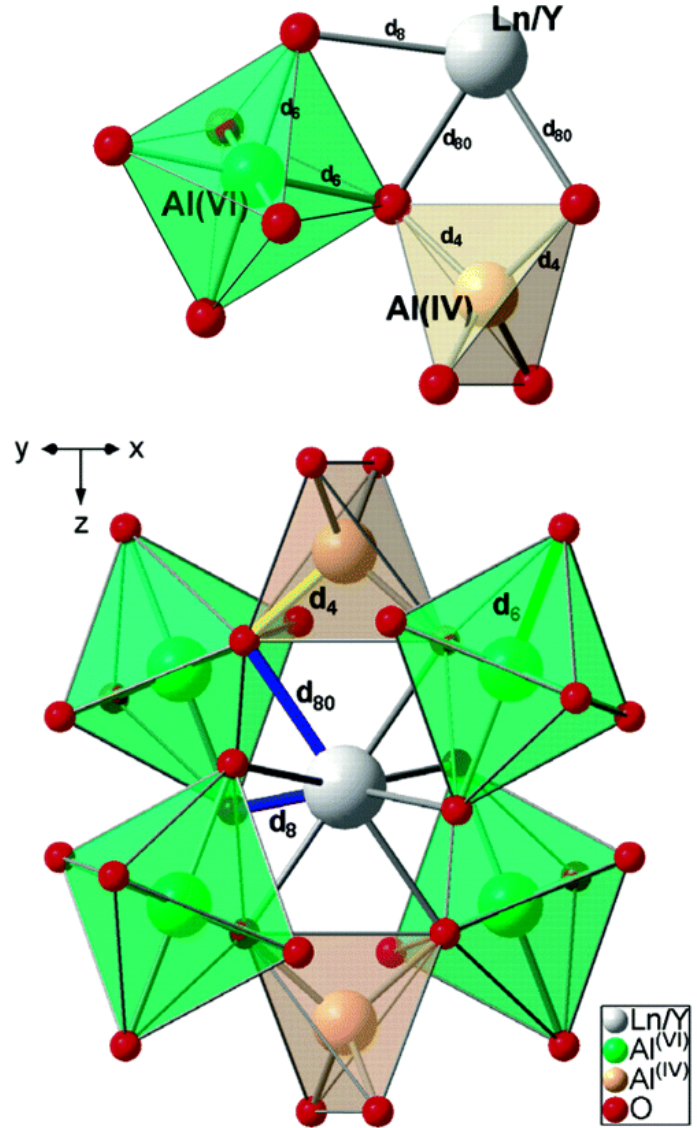


FIGURE 2. POLYHEDRA IN YAG [7] (with permission from the American Chemical Society)

The potential energy for any pair of atoms (ions), i and j , are given by the sum of a Coulombic and exponential term given by

$$U_{ij} = c \frac{q_i q_j}{r_{ij}} + A_{ij} \exp\left(-\frac{r_{ij}}{B_{ij}}\right) \quad (1)$$

where c is an energy conversion constant equal to $14.4 \text{ eV} \cdot \text{\AA} \cdot e^{-1}$.

In addition to pair potentials, three-body potentials were employed in order to impose angular bonding between certain triplets of atoms as seen in Fig. 2. For a triplet of atoms; i , j , and k ; the three-body interaction, U_{jik} , is expressed as

TABLE 2. TWO-BODY PARAMETERS

ij	$A_{ij}(\text{eV})$	$B_{ij}^{-1}(\text{\AA}^{-1})$	$q_i (e)$
O-O	2449.44	3.44	-2
Al-O	1740.31	3.44	+3
Y-O	1250.85	2.86	+3
Al-Al	312.11	14.06	
Y-Y	245.14	14.06	
Y-Al	256.55	14.06	

TABLE 3. THREE-BODY PARAMETERS

jik	$\lambda_{jik} (\text{eV})$	$\gamma (\text{\AA})$	$r_{0,ij} (\text{\AA})$	$\theta_{0,jik} (^\circ)$
Al/Y-O-Al/Y	6.242	2.0	2.6	109.5
O-Al-O	149.324	2.8	3.0	109.5
O-Y-O	168.250	2.8	3.0	109.5

$$U_{jik} = \begin{cases} \lambda_{jik} \exp\left(\frac{\gamma_{ij}}{r_{ij}-r_{ij,0}} + \frac{\gamma_{ik}}{r_{ik}-r_{ik,0}}\right) \Omega_{jik} & r_{ij} < r_{ij,0} \text{ and } r_{ik} < r_{ik,0} \\ 0 & r_{ij} \geq r_{ij,0} \text{ or } r_{ik} \geq r_{ik,0} \end{cases} \quad (2)$$

Ω_{jik} is an angular factor whose functional form depends on which triplet of atoms is being considered. For bonds where j and k represent oxygen atoms, and i represents an aluminum or yttrium atom (O-Al/Y-O), Ω_{jik} is expressed as

$$\Omega_{jik} = [(\cos \theta_{jik} - \cos \theta_{jik}^0) \sin \theta_{jik} \cos \theta_{jik}]^2. \quad (3)$$

For triplets Al/Y-O-Al/Y, Ω_{jik} is

$$\Omega_{jik} = (\cos \theta_{jik} - \cos \theta_{jik}^0)^2. \quad (4)$$

The parameters of Eqns. 2, 3, and 4 are in Tab. 3.

All simulations were performed using the June 5, 2010 version of the Large-scale Atomic/Molecular Massively Parallel Simulator (LAMMPS) package [11]. Furthermore, all simulations used the Verlet algorithm [12] for time integration. Also, periodic boundary conditions were imposed in all directions on all simulations to balance the repulsive forces from similarly charged two-body interactions.

The two-body interactions expressed by Eqn. 1 are implemented using the included Born-Mayer-Huggins potential [13] where the Coulombic interactions were computed in k-space.

However, in order to compute three-body energies and their forces for this work, code for two potentials was added based on the included Stillinger-Weber potentials (composed of two and three-body interactions). One implemented the three-body interaction formed by Eqn. 2 and Eqn. 3 while zeroing the original two-body interaction. The other involved only zeroing the two-body part of the Stillinger-Weber potentials since the three-body interaction formed by Eqn. 2 and Eqn. 4 is compatible with the original code.

Lattice Constant, Specific Heat Capacity, and Thermal Expansion from Simulated Heating

This section describes how the constant-pressure heat capacity, thermal expansion, and the lattice constant are found from simulated heating. These quantities are checked for dependence on temperature and x . Obtaining the lattice constant is necessary to perform the thermal conductivity simulations described in the next section.

Simulation Setup

a , c_p , and α are calculated from five simulations to represent a random aluminum substitution percentage of 0, 25, 50, 75, and 100 percent. The system size was 2x2x2 unit cells for all simulations. Each simulation was initialized with a gaussian velocity distribution giving a (translational) temperature of 10°K. Then, using NPT time integration, the system is thermostatted at 10°K and barostatted at 10 bars for 80,000 timesteps. Subsequently, the temperature is ramped by 100°K. After that, the system is again barostatted at 10 bars, thermostatted at the new temperature of 110°K, and time-integrated for another 80,000 timesteps. This process is repeated until the system reaches a temperature of 3000°K. Except for aluminum substitution, this simulation setup closely follows that of Ref. [10] to allow for comparison.

The simulations ran with a .002 ps timestep, 10^{-4} k-space precision, and a 7 Å cutoff (the cutoff is for two-body interactions). The damping parameter on the thermostat was 1 ps while the damping parameter on the barostat was 10 ps. An additional drag factor of 1 was imposed to dampen system oscillations.

A time series for the total energy, temperature, pressure, and the lattice constant was collected from the simulation by an averaging procedure: the quantities are sampled every 10 timesteps 100 times, and subsequently averaged. This average is then recorded.

Results and Discussion

The stability of kinetic energy in the simulation can be seen in the time series for temperature in Fig. 3. Variations in each temperature “step” were within 10°K while exhibiting almost no transients. Similarly, the lattice parameter, a , exhibited variations of 0.1% at most.

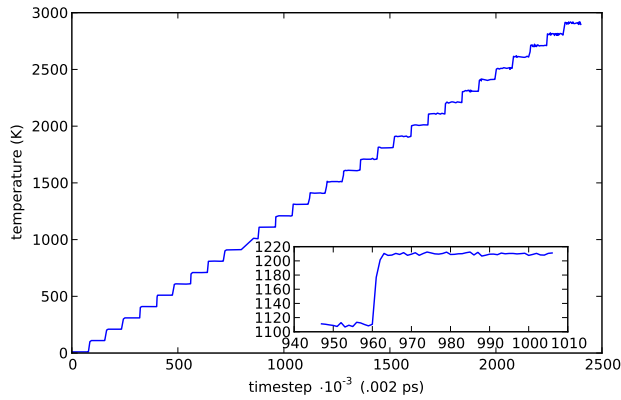


FIGURE 3. TEMPERATURE VS. TIME FOR 25% Al SUBSTITUTION

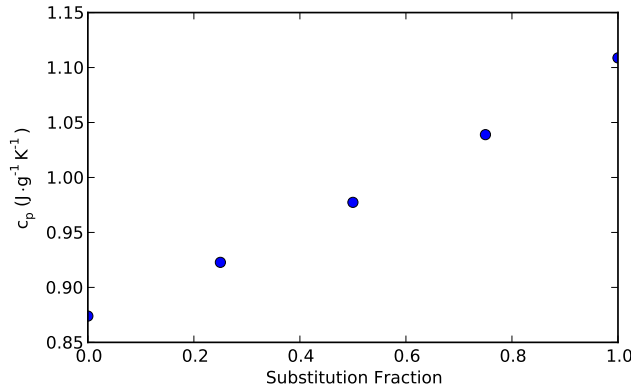


FIGURE 4. c_p VS. SUBSTITUTION FRACTION, x

Furthermore, there is a linear relationship between temperature and total energy for all simulations. c_p can then be computed using the slope of this relationship

$$c_p = \frac{\Delta E}{m\Delta T}. \quad (5)$$

Figure 4 shows c_p from all simulations. Given that $\Delta E/\Delta T$ were close to equal for all simulations, c_p is mostly a function of mass. However, the calculated c_p of pure YAG is about 40% over the experimental value of $0.6 \text{ J} \cdot \text{g}^{-1} \cdot \text{K}^{-1}$.

Similarly, a linear relationship was also found between temperature and lattice constant for all simulations. α can be found

using the slope of this relationship

$$\alpha = \frac{\Delta V}{V_0 \cdot 3\Delta T}. \quad (6)$$

However, α was $7.8 \cdot 10^{-6} \text{ K}^{-1}$ for all simulations showing no dependence on aluminum substitution. This is expected given that the potential energy functions were the same for the substituted atoms. Nonetheless, this compares well with the established figure of $7.0 \cdot 10^{-6} \text{ K}^{-1}$ for pure YAG. As a result, the lattice constant, a , was taken to be only a function of temperature expressed in angstroms as

$$a = 9.67 \cdot 10^{-5} T \frac{\text{\AA}}{\text{K}} + 12.4 \text{\AA}. \quad (7)$$

So at 300°K , the lattice constant is 12.43\AA which is 3.6% over published figures [8] but only 0.6% over the result from MD simulations of Ref. [10].

The validity of α and a for gallium-substituted YAG can be questioned since they have not been verified by experiment.

Thermal Conductivity from Non-Equilibrium Simulations

The simulations described in this section measure thermal conductivity in the $[1 \ 0 \ 0]$ direction. Since YAG is arranged in a cubic structure, its thermal conductivity is given by a diagonal tensor

$$k_{ij} = \begin{vmatrix} k & 0 & 0 \\ 0 & k & 0 \\ 0 & 0 & k \end{vmatrix}. \quad (8)$$

Therefore, the thermal conductivity tensor is fully described by this one measure.

k is obtained by imposing a temperature gradient so that Fourier's law of conduction in one dimension (Eqn. 9) may be evaluated directly.

$$k = -\dot{q}_x \frac{dx}{dT} \quad (9)$$

Simulation Setup

Two temperature gradients were imposed in a symmetric configuration, as represented in Fig. 5, since the simulations feature periodic boundary conditions. This configuration ensures

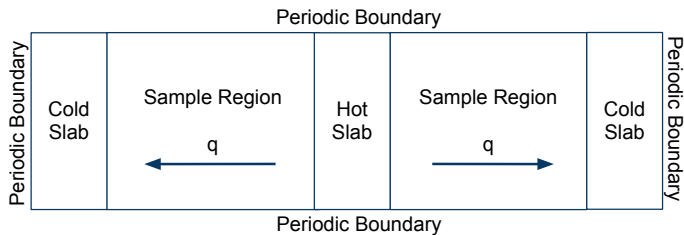


FIGURE 5. NON-EQUILIBRIUM MD CONFIGURATION

that the hot slab is not exposed to the cold slab at the simulation boundary.

For all simulations, the lattice spacing was 12.43 Å. Furthermore, the hot slab was 8x1x1 (WxHxD) unit cells, while each cold slab was 4x1x1 unit cells. As such, the atoms in each 4x1x1 region were assigned to four thermostats. The thermostats were applied to the hot slab and cold slab such that the average temperature of the temperature gradient was 300°K. Additionally, the temperature difference between the thermostats was fixed at 40°K for all simulations.

However, the simulations were varied in the size of the “sample region” and in random aluminum substitution fraction, x . The sample sizes were 4, 8, 16, and 32; while x was 0, 50, and 100 percent, giving a total of 12 simulations.

An initial linear temperature gradient was imposed over the sample region with a random gaussian velocity distribution. The temperature gradient is then maintained by the thermostats for 1000 timesteps times the system size in unit cells to achieve steady state. The region controlled by the thermostats are time-integrated with the NVT integrator, while the sample region was time-integrated with the NVE integrator. Subsequently, the simulations ran for at least 0.2 fs to at most 2.5 fs, depending on the amount of time necessary to minimize short term energy fluctuations.

During the run, the average temperature in each unit cell is calculated every 10 timesteps. The time average is then recorded for 100 of these calculations. Meanwhile, the data from the thermostats are recorded every 1000 timesteps. The data from the thermostats represent the cumulative energy change of the system due to their action. In particular, here it represents an energy addition or subtraction due to the flow of energy from the hot slab to the cold slab.

The following tabulates the simulation settings. The cutoffs apply to the two-body potential (Eqn. 1).

timestep	.001 ps
exp. term cutoff	4.0 Å
Coulombic term cutoff	7.0 Å
k-space precision	10^{-5}
thermostat damping	1 ps

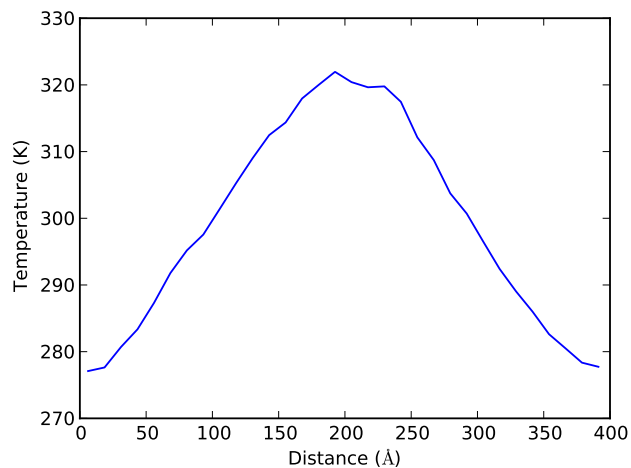


FIGURE 6. AVERAGE TEMPERATURE PROFILE FOR A SAMPLE SIZE 8 UNIT CELLS WIDE, WITH 50% Al SUBSTITUTION, AVERAGED OVER .618 ns

Results and Discussion

Figure 6 typifies the temperature profile found in all simulations when averaged over their run time.

To calculate thermal conductivity according to Fourier’s law (Eqn. 9), the slope from a line fit to the sample region from each side of the temperature profile is averaged to obtain $\Delta x/\Delta T$. In addition, q_x is $\Delta E/\Delta t$ where ΔE is represented by the energy difference of E_{th}^{avg} between the start and end of the simulation in steady state.

Figure 7 shows the results of the thermal conductivity calculation. For pure YAG, the trend is approaching (the lower end of) its accepted bulk value of $10 \text{ W}\cdot\text{m}^{-1}\text{K}^{-1}$ [6]. All trends of a certain substitution fraction (varying system size) can be explained by simplified kinetic theory: the relationship between thermal conductivity, specific heat capacity, group velocity, and mean free path is given by

$$k = \frac{1}{3} v \Lambda c_v. \quad (10)$$

Since system size is the only variable, the decrease in thermal conductivity with decreasing system size is due to decreased mean free path.

Meanwhile, group velocity is needed to fully explain the trends for a certain system size (varying substitution fraction). Nonetheless, assuming acoustic phonons are the primary thermal carriers, the lower thermal conductivity of YAG fully substituted with gallium compared to pure YAG can be explained by the difference in their phonon dispersions: as gallium is a heavier element than aluminum, the group velocity of fully substituted

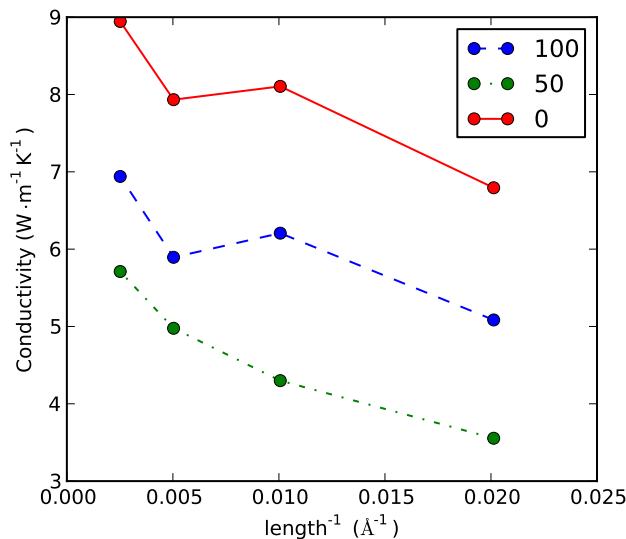


FIGURE 7. THERMAL CONDUCTIVITY TRENDS FOR $x = 0, 50,$ AND 100%

YAG will be lower, resulting in lower thermal conductivity. Still, decreased mean free path explains why the thermal conductivity for $x=50\%$ is less than $x=0\%$ and $x=100\%$.

Conclusions

The model for pure YAG shows good agreement with experimental values for constant-pressure specific heat, thermal expansion, and thermal conductivity at 300°K . The relationship between thermal conductivity and aluminum substitution is not monotonic. Furthermore, experimental thermal properties for gallium-substituted YAG are needed to confirm the YAG model used in this work.

REFERENCES

- [1] Hansel, R., Allison, S., and Walker, G., 2010. "Temperature-dependent luminescence of gallium-substituted YAG:Ce". *Journal of Materials Science*, **45**, pp. 146–150. 10.1007/s10853-009-3906-9.
- [2] Caslavsky, J. L., and Viechnicki, D. J., 1980. "Melting behaviour and metastability of yttrium aluminium garnet (YAG) and YAlO_3 determined by optical differential thermal analysis". *Journal of Materials Science*, **15**, pp. 1709–1718. 10.1007/BF00550589.
- [3] Wynne, R., Daneu, J. L., and Fan, T. Y., 1999. "Thermal coefficients of the expansion and refractive index in YAG". *Appl. Opt.*, **38**(15), pp. 3282–3284.
- [4] Red Optronics. Undoped yag crystal (Y3Al5O12). On the

WWW. URL <http://www.redoptronics.com/undoped-YAG-crystal.html>.

- [5] Qiu, H., Yang, P., Dong, J., Deng, P., Xu, J., and Chen, W., 2002. "The influence of Yb concentration on laser crystal Yb:YAG". *Materials Letters*, **55**(1-2), pp. 1 – 7.
- [6] Morikawa, J., Leong, C., Hashimoto, T., Ogawa, T., Urata, Y., Wada, S., Higuchi, M., and ichi Takahashi, J., 2008. "Thermal conductivity/diffusivity of Nd^{3+} doped GdVO_4 , YVO_4 , LuVO_4 , and $\text{Y}_3\text{Al}_5\text{O}_{12}$ by temperature wave analysis". *Journal of Applied Physics*, **103**(6), p. 063522.
- [7] Dobrzycki, L., Bulska, E., Pawlak, D. A., Frukacz, Z., and Wozniak, K., 2004. "Structure of YAG crystals doped/substituted with erbium and ytterbium". *Inorganic Chemistry*, **43**(24), pp. 7656–7664. PMID: 15554630.
- [8] Bodzenta, J., Kaźmierczak-Bałata, A., Wokulska, K. B., Kucytowski, J., Łukasiewicz, T., and Hofman, W., 2009. "Influence of doping on thermal diffusivity of single crystals used in photonics: measurements based on thermal wave methods". *Appl. Opt.*, **48**(7), pp. C46–C54.
- [9] Jmol: an open-source java viewer for chemical structures in 3d. On the WWW. URL <http://www.jmol.org/>.
- [10] Jun, C., Dong-Quan, C., and Jing-Lin, Z., 2007. "Molecular dynamics simulation of thermodynamic properties of YAG". *Chinese Physics*, **16**(9), p. 2779.
- [11] Plimpton, S., 1995. "Fast parallel algorithms for short-range molecular-dynamics". *JOURNAL of Computational Physics*, **117**(1), MAR 1, pp. 1–19.
- [12] Verlet, L., 1968. "Computer "experiments" on classical fluids. ii. equilibrium correlation functions". *Phys. Rev.*, **165**(1), Jan, pp. 201–214.
- [13] Tosi, M. P., and Fumi, F. G., 1964. "Ionic sizes and born repulsive parameters in the nacl-type alkali halides—ii : The generalized huggins-mayer form". *Journal of Physics and Chemistry of Solids*, **25**(1), pp. 45 – 52.